Infacon XV: International Ferro-Alloys Congress, Edited by R.T. Jones, P. den Hoed, & M.W. Erwee,
Southern African Institute of Mining and Metallurgy, Cape Town, 25–28 February 2018

Reduction rates of MnO and SiO_2 in SiMn slags between 1500 and 1650°C

P.P. Kim, T.A. Larssen, and M. Tangstad
Department of Materials Science and Engineering,
Norwegian University of Science and Technology, Trondheim, Norway

Abstract – The kinetics of MnO and SiO_2 reduction in SiMn slags based on Assmang / Comilog ore and high-carbon ferromanganese (HCFeMn) slag were investigated between 1500 and 1650°C under CO atmosphere. The results showed that charges containing HCFeMn slag had relatively faster reduction rates than the charges without. The difference in the driving force for MnO reduction was insignificant between the SiMn slags at 1500°C, which implied a low contribution of the driving force for reduction rate. The comparison of slag viscosities was also rather similar at 1500°C, which could not explain the different reduction rates. Different charges will contain various sulfur contents, and it is believed that this is the main source of variation in the reduction rates. The estimated activation energies for MnO reduction were around 500–920 kJ/mol for charges containing HCFeMn slag and between 250–300 kJ/mol without. Based on the estimated kinetic parameters, the considered rate models were able to describe the reduction of MnO and SiO_2 in SiMn slags between 1500 and 1650°C.

Keywords: SiMn, MnO, SiO_2, reduction, kinetics, slag

INTRODUCTION

Manganese ferro-alloys, such as ferromanganese (FeMn) and silicomanganese (SiMn), are important ingredients for steel production, due to their many contributions. Mn enhances the strength, toughness, and hardness of steel products, and both Mn and Si are used as deoxidizers to prevent porous structures (International Manganese Institute, 2014; Olsen, Tangstad, & Lindstad, 2007; Subramanyam, Swansiger, & Avery, 1990; Tomota *et al.*, 1987).

The thermodynamic background of manganese ferro-alloys is well established (Olsen, Tangstad, & Lindstad, 2007), but kinetic information is rather scarce, especially for the SiMn process (Tranell *et al.*, 2007; Tore-Andre Skjervheim, 1994). The absence of kinetic information makes it more difficult to understand the reduction mechanisms of MnO and SiO_2. It is not clear how different raw materials affect the SiMn process. The main metal-producing reactions in the SiMn process are described by the following reactions [1] and [2]:

$$MnO_{(l)} + C = Mn_{(l)} + CO_{(g)} \quad [1]$$

$$SiO_{2\,(l)} + 2C = Si_{(l)} + 2CO_{(g)} \quad [2]$$

Recent studies have observed that both MnO and SiO_2 are reduced to Mn and Si significantly above 1500°C (Kim *et al.*, 2016; Kim *et al.*, 2017). The mass change observed from a TGA furnace was low until 1500°C, but increased significantly at higher temperatures. It was perceived that most of the MnO and SiO_2 reduction had occurred between 1500 and 1650°C, but the reasons were not fully understood. Therefore, the present study focuses on the kinetic information of MnO and SiO_2

reduction in the SiMn slags (MnO-SiO_2-CaO-MgO-Al_2O_3) between 1500 and 1650°C, using different sources of Mn.

THEORETICAL CONSIDERATIONS

The reduction rate of MnO was studied previously and was described by Equation [3] (Olsen, Tangstad, & Lindstad, 2007; Ostrovski *et al.*, 2002). This equation is based on the FeMn process, and implies that the chemical reaction is the rate determining step. As SiMn slags are essentially similar to FeMn slags, Equation [3] can also be used for MnO reduction in SiMn slags. For SiO_2, a recent study has shown that the dissolution of SiO_2 into slag was the rate determining step (Maroufi *et al.*, 2015). However, opposite results have also been observed where the dissolution of both MnO and SiO_2 into slag were completed before significant reduction above 1500°C (Kim *et al.*, 2018*; Holtan, 2015). In this study, a similar rate equation for SiO_2 reduction was presumed by Equation [4], assuming SiO_2 reduction is also controlled mainly by chemical reaction. Both Equations [3] and [4] were considered in this work to estimate the kinetic parameters.

$$r_{MnO} = k_{MnO} \cdot A \cdot (a_{MnO} - a_{MnO,Eqm.}) = k_{o,MnO} \cdot A \cdot e^{-E_{MnO}/RT} \cdot (a_{MnO} - \frac{a_{Mn}}{K_{T,MnO}}) \quad [3]$$

$$r_{SiO_2} = k_{SiO_2} \cdot A \cdot (a_{SiO_2} - a_{SiO_2,Eqm.}) = k_{o,SiO_2} \cdot A \cdot e^{-E_{SiO_2}/RT} \cdot (a_{SiO_2} - \frac{a_{Si}}{K_{T,SiO_2}}) \quad [4]$$

where r is the reduction rate (g/min), k is the rate constant (g/min·cm²), k_o is the frequency factor, A is the reaction area (cm²), E is the activation energy (kJ/mol), R is the gas constant, T is the temperature, a_{MnO}, a_{SiO2} are the activities of MnO and SiO_2 in the slag phase, $a_{MnO,Eqm.}$, $a_{SiO2,\ Eqm.}$ are the activities of MnO and SiO_2 at equilibrium, and K_T is the equilibrium constant at temperature T.

The considered rate models for MnO and SiO_2 reduction also imply that the driving force, which is the difference between the activity of slag (MnO, SiO_2) and produced metal (Mn, Si), contribute to the reduction rates. The simplified models for activities of slag and metal have been studied recently (Olsen, 2016). These activities were based on FactSage 7.0 (CRCT and GTT, 2015), and thermodynamic data from HSC Chemistry 7 (Outotec) was used to calculate the driving forces of MnO and SiO_2 reduction at different temperatures.

EXPERIMENTAL PROCEDURES

The chemical compositions of raw materials are shown in Table I, and the SiMn charges are described in Table II. Three different Mn-sources – Assmang ore, Comilog ore, and HCFeMn slag – were used to study different SiMn charges in this work. The sizes of the raw materials were between 0.6 and 1.6 mm. Each raw material was weighed to aim at approximately 40 wt% SiO_2 in slag and 18 wt% Si in the metal phase, which is close to the thermodynamic equilibrium at 1600°C (Olsen, Tangstad, & Lindstad, 2007). The charge materials were added into graphite crucibles (36 mm outer diameter, 30 mm inner diameter, 70 mm height, and 61 mm deep).

Table I: Chemical composition of raw materials

Material	MnO	MnO_2	SiO_2	Fe_2O_3	CaO	MgO	Al_2O_3	S	C	CO_2	H_2O	Total [wt%]
Assmang	32.7	33.2	5.8	15.1	6.3	1.1	0.3	0.16	0.3	3.5	1.6	100.6
Comilog	3.0	72.4	4.6	6.7	0.1	0.1	5.6	-	-	0.1	5.0	97.6
Quartz	0.1	-	93.9	-	0.1	0.1	1.2	-	-	-	-	95.4
HCS*	35.2	-	25.5	-	18.5	7.5	12.3	0.46	0.4	-	2.2	102.1
Coke	-	-	5.6	0.86	0.4	0.2	2.8	0.4	87.7	-	15.5	113.5

* HCS: High-Carbon FeMn Slag

Table II: SiMn charges used in the experiments

Charge	Assmang*	Comilog*	Quartz	HCS*	Coke	Total [g]
As	7	-	1.9	-	2.2	11.1
As/HCS	4	-	1.7	4	2.5	12.2
Com	-	6	1.4	-	2.0	9.4
Com/HCS	-	4	1.6	4	2.3	11.9
HCS	-	-	1.5	10	3.0	14.5

* Mn bearing materials

The TGA furnace, which is schematically described in Figure 1, was used to conduct the experiments. The furnace can endure temperatures up to 1700°C, and the maximum heating rate is up to 25°C/minute. A mass balance is installed at the top, and a molybdenum (Mo) wire was used to suspend the graphite crucible inside the chamber. The temperature schedule of the experiment was considered to simulate an industrial furnace operation and is described in Figure 2. Initially, the furnace was rapidly heated up to 1200°C (+25°C/minute) and held for 30 minutes to secure a complete degree of pre-reduction (Olsen, Tangstad, & Lindstad, 2007). Then, further heating (+4.5°C/minute) was done and stopped at targeted temperatures between 1500 and 1650°C. All experiments were conducted in CO at atmospheric pressure.

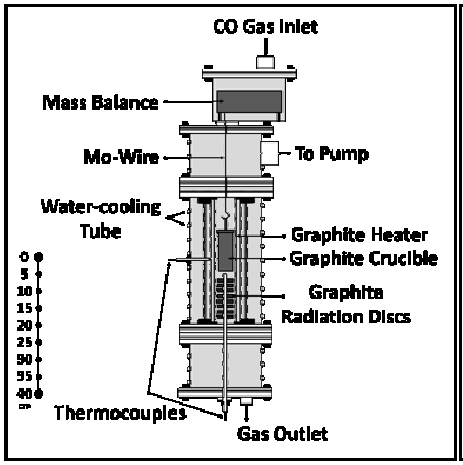

Figure 1: Schematic of the TGA furnace

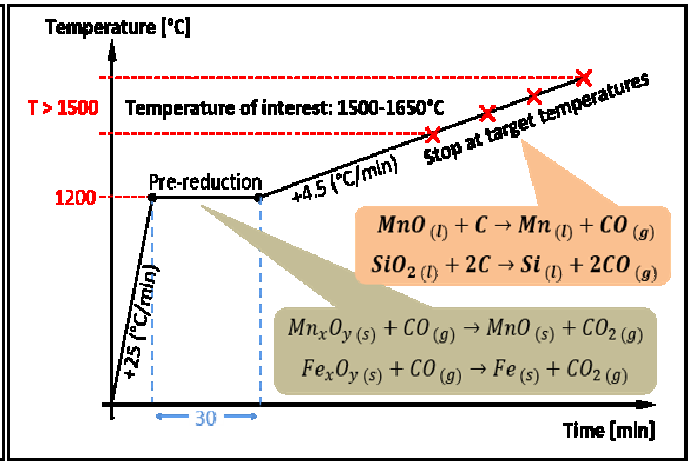

Figure 2: The temperature schedule

The weight loss of each charge samples was recorded and data were logged every 5 seconds during the experiment. Lastly, each charge sample was prepared by mounting it in epoxy to be further analyzed. EPMA (Electron Probe Micro Analyzer) was done by using JEOL JXA-8500F to analyze the slag compositions. The average slag composition from more than 5 analyzed points were used to calculate the metal composition (as the metal analyses are more uncertain than the slag analyses).

RESULTS AND DISCUSSION

The mass change from the TGA furnace during the experimental condition is the main information. Figure 3 describes the TGA results of different SiMn charges between 1200 and 1650°C. Note that a complete degree of pre-reduction was assumed at 1200°C, and used as a new reference point for further reduction of MnO and SiO_2. The mass changes for all SiMn charges were insignificant below 1500°C, which indicated a low degree of MnO and SiO_2 reduction. The reduction rate increased above 1500°C, which is in accordance with previous studies (Kim *et al.*, 2016; Kim *et al.*, 2017), but the degree of reduction differed with different SiMn charges. It was observed that charges containing HCFeMn slag resulted in faster and higher degrees of reduction. Although the apparent effect of accelerated reduction can be thought to be from the use of HCFeMn slag, the TGA results do not necessarily describe the degrees of reduction of MnO and SiO_2 separately. Quantitative slag and metal analyses are required for further information.

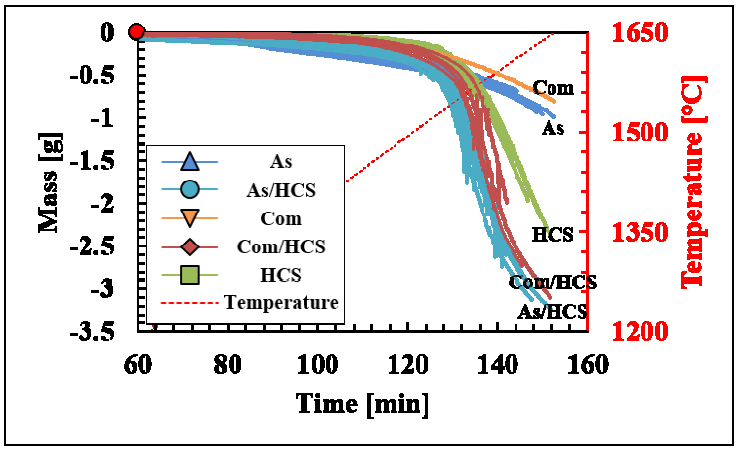

Figure 3: TGA results: Several experiments for each charge between 1500 and 1650°C with a new reference point (red circle) at 1200°C

The average slag and metal compositions with their respective activities (slag: a_{MnO} and a_{SiO2}, metal: a_{Mn}/K_T and a_{Si}/K_T) between 1500 and 1650°C of the different charges are shown in Table III. Significant reduction of MnO was clearly observed with charges containing HCFeMn slag. The MnO content of slag between 1500 and 1650°C for charges 'As/HCS' and 'HCS' decreased from approximately 40 and 31 wt% to 5 and 7 wt%, respectively. A similar degree of reduction was also observed from charge 'Com/HCS', where the decrease of MnO was approximately 43 to 6 wt% between 1500 and 1650°C. On the other hand, charges without HCFeMn slag, 'As' and 'Com', showed the opposite results. The MnO contents were still relatively high compared to the charges containing HCFeMn slag. This shows good accordance with the TGA results in Figure 3, where it implies that most of the mass change was due to MnO reduction between 1500 and 1650°C.

Table III: Analysed slag and calculated metal compositions with their respective activities between 1500 and 1650°C

Charge-Temp.	Slag (EPMA) [wt%]								Metal (Calculated) [wt%]					
	MnO	SiO_2	CaO	MgO	Al_2O_3	a_{MnO}	a_{SiO2}	C+M/A	Mn	Si	Fe	C	a_{Mn}/K_T	a_{Si}/K_T
As-1500	50.6	39.1	7.6	1.2	0.5	0.152	0.285	17.2	54.6	4.3	35.9	5.2	0.0037	0.1280
1510	49.3	40.5	7.7	1.3	0.7	0.137	0.339	13.7	55.9	2.0	35.9	6.2	0.0035	0.0378
1520	51.3	37.9	7.2	1.3	0.5	0.171	0.237	16.0	54.4	7.4	34.0	4.2	0.0030	0.1914
1530	50.5	38.8	7.7	1.2	0.5	0.160	0.269	16.4	55.2	5.8	34.3	4.6	0.0029	0.0994
1540	51.4	37.4	8.4	0.7	0.7	0.181	0.218	13.3	55.0	8.8	32.6	3.5	0.0026	0.1598
1550	50.1	38.7	8.3	0.8	0.7	0.165	0.258	12.7	56.4	7.4	32.2	4.1	0.0025	0.0915
1560	50.8	37.9	7.5	1.4	0.5	0.177	0.229	16.3	55.8	8.7	31.7	3.8	0.0021	0.1026
1570	49.0	39.7	7.7	1.3	0.5	0.155	0.289	16.6	57.6	6.7	31.3	4.5	0.0021	0.0504
1580	49.4	39.0	8.6	0.7	0.8	0.165	0.261	11.7	57.5	8.1	30.6	3.9	0.0019	0.0543
1590	50.1	38.2	8.9	0.8	0.7	0.179	0.230	13.4	57.1	9.4	30.1	3.4	0.0017	0.0587
1600	49.1	38.7	8.9	0.7	0.9	0.173	0.243	11.1	58.3	9.7	28.6	3.5	0.0016	0.0511
1610	48.4	38.8	9.1	0.7	0.8	0.173	0.240	12.5	59.1	10.4	27.3	3.2	0.0015	0.0479
1620	48.7	37.7	9.4	0.7	0.9	0.193	0.198	11.0	59.2	12.3	25.8	2.7	0.0013	0.0581
1630	46.1	40.5	8.0	1.4	0.8	0.154	0.289	11.6	60.8	9.9	25.6	3.6	0.0013	0.0311
1640	45.7	40.1	9.3	1.4	0.8	0.162	0.263	13.3	61.1	11.3	24.3	3.3	0.0011	0.0339
1650	48.1	37.3	7.5	1.3	0.7	0.208	0.175	12.0	59.6	13.5	24.2	2.8	0.0009	0.0443
As/HCS-1500	40.5	35.1	12.3	3.8	5.2	0.210	0.107	3.1	50.0	10.7	36.5	2.9	0.0031	0.6101
1510	39.8	35.4	12.2	3.5	5.8	0.204	0.111	2.7	52.7	10.6	33.8	3.0	0.0030	0.4818
1520	39.1	36.6	12.0	3.9	5.6	0.184	0.135	2.9	54.5	5.2	35.6	4.7	0.0032	0.1010
1530	39.1	35.7	12.1	3.7	4.9	0.200	0.113	3.3	54.6	10.5	31.8	3.1	0.0026	0.2934
1540	38.3	36.8	12.2	3.9	5.0	0.182	0.135	3.2	56.8	6.4	32.4	4.4	0.0028	0.0904
1550	34.1	39.0	13.2	3.7	6.3	0.143	0.168	2.7	64.8	6.5	24.1	4.6	0.0029	0.0734
1560	29.5	40.4	14.4	4.0	6.7	0.115	0.182	2.7	68.4	8.9	18.7	3.9	0.0027	0.1021
1570	24.0	41.8	16.2	4.3	8.0	0.087	0.187	2.6	70.2	11.1	15.3	3.4	0.0024	0.1244
1580	19.7	44.1	18.3	5.2	8.8	0.062	0.227	2.7	72.0	10.3	14.1	3.7	0.0023	0.0838
1590	17.2	44.2	19.2	5.2	9.2	0.054	0.212	2.7	71.8	11.6	13.2	3.4	0.0020	0.0882
1600	12.7	43.8	21.6	6.2	10.4	0.039	0.174	2.7	71.3	13.9	12.0	2.9	0.0016	0.1094
1610	12.3	45.4	21.2	6.0	10.7	0.035	0.213	2.6	72.2	12.4	12.1	3.2	0.0016	0.0682
1620	10.9	44.6	22.5	6.4	11.5	0.032	0.183	2.5	71.6	13.7	11.7	3.0	0.0014	0.0710
1630	6.8	45.5	24.2	6.7	12.4	0.018	0.181	2.5	71.8	14.1	11.1	2.9	0.0013	0.0637
1640	6.8	44.0	24.9	7.2	12.8	0.020	0.147	2.5	71.0	15.2	11.0	2.8	0.0011	0.0651
1650	4.9	43.9	26.5	7.1	13.8	0.014	0.136	2.4	70.9	15.7	10.7	2.8	0.0010	0.0591
HCS-1500	31.7	34.5	15.4	4.9	9.4	0.171	0.076	2.2	27.3	30.1	36.2	6.4	0.0005	-
1510	31.7	34.2	15.8	5.0	9.7	0.176	0.072	2.2	29.7	32.4	27.2	10.7	0.0002	-
1520	31.5	34.1	15.9	5.1	9.7	0.178	0.069	2.2	35.5	32.1	22.2	10.2	0.0002	-
1530	30.8	33.8	15.8	5.2	10.0	0.179	0.064	2.1	43.8	31.5	15.0	9.6	0.0001	-
1540	31.7	34.4	15.8	5.5	9.2	0.177	0.074	2.3	28.6	30.7	33.2	7.6	0.0002	-
1550	30.6	35.8	16.1	5.6	9.5	0.155	0.092	2.3	58.6	0.1	34.5	6.9	0.0027	-
1560	30.0	35.7	16.3	5.8	9.7	0.154	0.090	2.3	63.9	8.8	23.5	3.9	0.0025	0.1012
1570	27.6	35.6	16.9	5.8	10.0	0.143	0.080	2.3	68.5	18.9	10.1	2.5	0.0013	0.5175
1580	24.1	38.8	17.3	5.5	11.3	0.098	0.124	2.0	82.1	3.4	8.2	6.3	0.0028	0.0126
1590	23.7	38.4	17.5	5.8	11.4	0.100	0.116	2.1	80.5	7.0	7.6	5.0	0.0025	0.0302
1600	21.2	38.8	18.5	6.2	11.5	0.086	0.114	2.2	79.9	10.4	5.9	3.9	0.0021	0.0507
1610	17.1	40.1	19.4	6.3	12.9	0.061	0.124	2.0	80.8	10.8	4.6	3.8	0.0019	0.0444
1620	14.3	40.8	21.3	6.8	13.3	0.047	0.127	2.1	80.8	11.6	4.0	3.7	0.0017	0.0423
1630	11.6	41.5	22.9	7.1	13.9	0.035	0.130	2.2	80.8	12.1	3.6	3.6	0.0016	0.0385
1640	9.2	40.2	23.6	7.8	15.3	0.028	0.097	2.0	77.7	16.4	3.2	2.9	0.0010	0.0694
1650	7.1	40.2	25.5	7.8	15.9	0.021	0.092	2.1	77.3	17.0	3.0	2.8	0.0009	0.0657
Com-1500	62.4	28.8	0.1	0.2	2.5	0.306	0.106	0.1	51.8	14.3	31.7	2.2	0.0028	1.2916
1550	57.9	30.4	0.3	0.2	4.4	0.264	0.136	0.1	66.3	15.0	16.2	2.5	0.0022	0.4250
1600	54.7	30.0	0.4	0.2	5.3	0.242	0.138	0.1	68.8	16.5	12.2	2.5	0.0013	0.1802
1650	49.7	35.5	0.3	0.2	5.6	0.161	0.261	0.1	71.8	12.9	12.1	3.2	0.0012	0.0359
Com/HCS-1550	43.1	33.9	9.0	3.6	7.4	0.220	0.113	1.7	61.7	9.8	25.0	3.5	0.0026	0.1588
1580	26.2	41.3	13.0	4.4	11.8	0.077	0.225	1.5	78.4	9.9	7.8	4.0	0.0025	0.0714
1600	19.0	43.0	14.7	5.1	14.2	0.045	0.234	1.4	78.3	11.9	6.4	3.5	0.0020	0.0694
1630	10.4	43.3	19.0	6.5	17.7	0.019	0.200	1.4	77.0	14.6	5.4	3.0	0.0013	0.0638
1650	5.7	40.9	22.2	7.6	20.6	0.009	0.134	1.5	75.1	17.1	5.0	2.8	0.0026	0.1588

The a_{MnO} also represents the reduction of MnO for all charges. Figure 4 compares the a_{MnO} for all charges between 1500 and 1650°C. Note that each point represents an experiment. The a_{MnO} for all the charges was similar at 1500°C: approximately 0.2 (1550°C for 'Com/HCS'). Only charges containing HCFeMn slag have dropped down near to 0 at 1650°C, which also indicates a higher degree of MnO reduction. This implies that the driving force for MnO reduction ($a_{MnO} - a_{Mn} \approx a_{MnO}$) will have insignificant impact on the reduction rate according to Equations [3] and [4] in the start of reduction. Therefore, it is not the driving force, but the rate constant that differs more between the different charges.

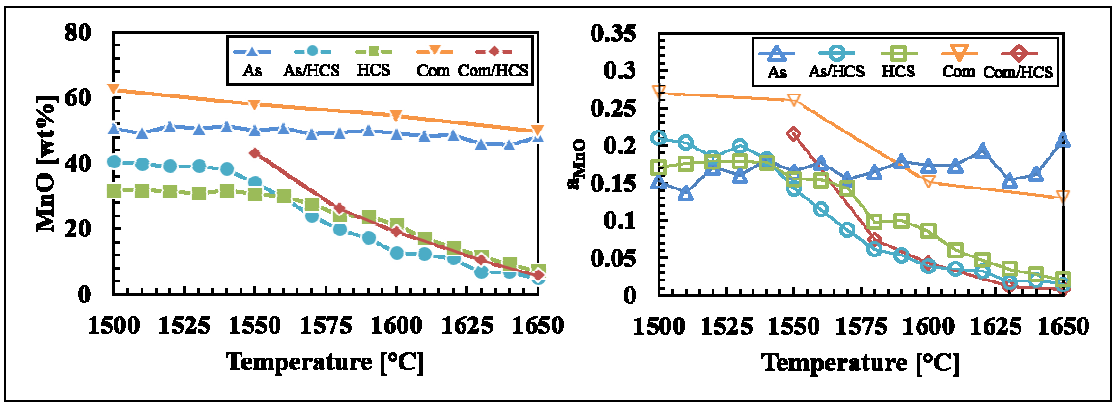

Figure 4: Comparison of MnO (left) and a_{MnO} (right) between 1500 and 1650°C

The rate constants in this study are expressed in relation to the Arrhenius equation according to Equations [3] and [4]. The Arrhenius plots of MnO and SiO_2 reduction for all charges are described in Figure 5, and the estimated activation energies are shown in Table IV. The Arrhenius plot for MnO reduction shows that charges containing HCFeMn slag have higher rate constants with increasing temperature. Also, the temperature dependency (activation energy) seems to be similar with different charge types: Charges including HCFeMn slag ('As/HCS', 'Com/HCS', and 'HCS') were approximately between 500 and 920 kJ/mol, and charges without HCFeMn slag ('As' and 'Com') were between 250 and 300 kJ/mol. The Arrhenius plot for SiO_2 reduction was difficult to estimate due to the small amount of Si produced. However, the temperature dependencies for SiO_2 reduction were somewhat similar within the experimental condition.

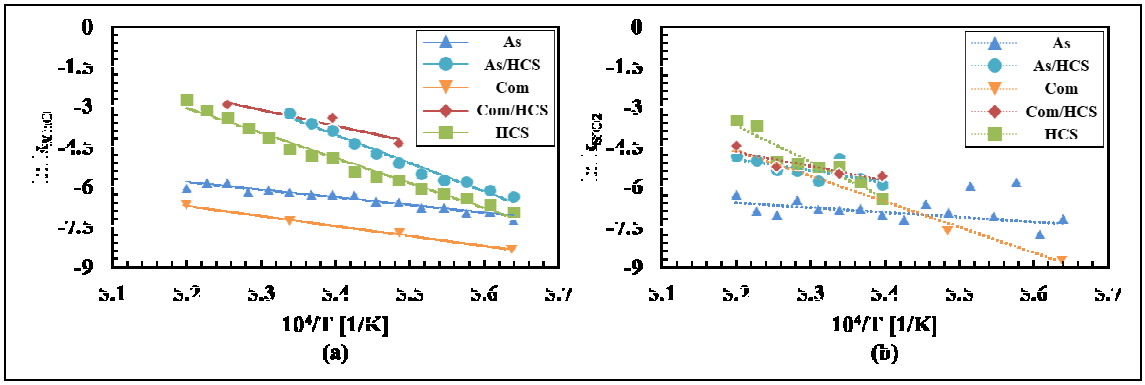

Figure 5: Arrhenius plots of MnO reduction (a) and SiO_2 reduction (b) between 1500 and 1650°C

Table IV: Summary of the estimated activation energies for MnO and SiO_2 reduction between 1500 and 1650°C

Charge	MnO Reduction [kJ/mol]	SiO_2 Reduction [kJ/mol]
As	250	160
As/HCS	920	870
Com	305	450
Com/HCS	500	790
HCS	780	1130

As the main difference between the different charges is the rate constant, the rate constants for MnO reduction are compared with the viscosity of the slag in Figure 6. If the assumption of chemical reaction being rate determining is not valid, the viscosity could affect the rate. The viscosities were calculated by using FactSage 7.0 (CRCT and GTT, 2015). No correlation with the viscosity of the slag in the initial phase of the reduction was found, and the rate constant is hence not affected by the viscosity in the slag, and probably neither the diffusion, which can be correlated with viscosity.

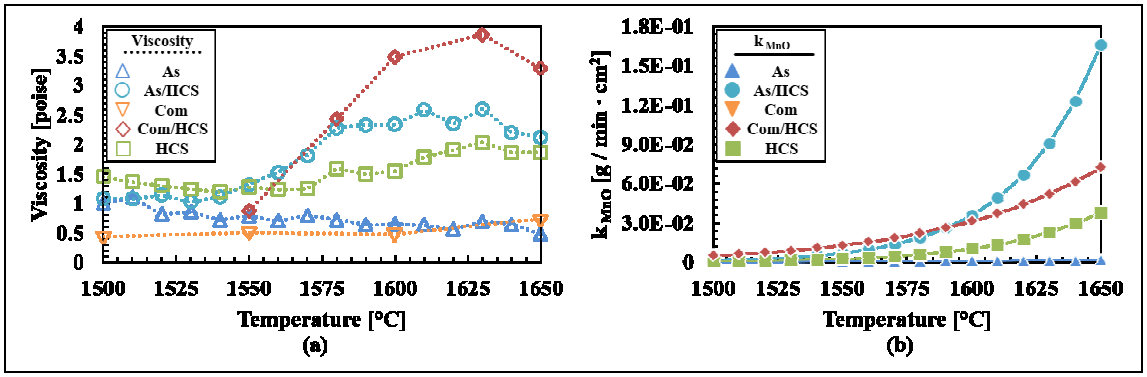

Figure 6: Comparison of slag viscosity (a) and rate constants (b) (MnO reduction) between 1500 and 1650°C

Sulfur is known to behave as a strong surface-active species for most metals (Stølen & Grande, 2004). The comparison of the initial amount of sulfur in the charge and the rate constants (MnO reduction) between 1500 and 1650°C is shown in Figure 7. Note that the amount of sulfur was calculated from the raw materials excluding coke. It is seen that the rate constant increases with the sulfur content and then decreases again. This is in accordance with previous observations where the sulfur content was studied separately (Kim *et al.*, 2018*; Kawamoto, 2016; Larrsen, 2016).

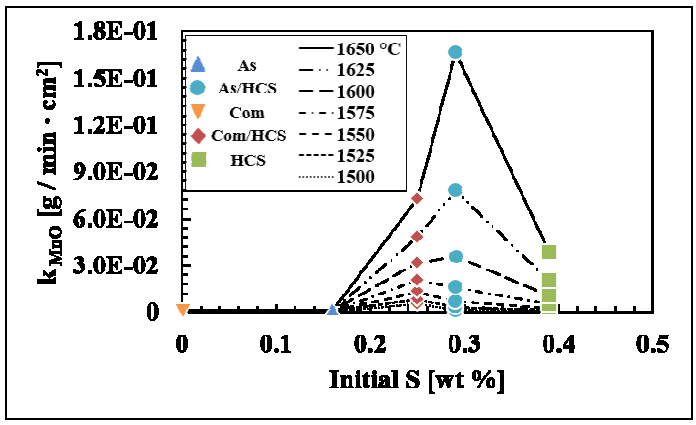

Figure 7: Comparison of initial amount of sulfur in charge and rate constants (MnO reduction) between 1500 and 1650°C

By applying the estimated kinetic parameters in Figure 5, the changing amount of MnO and SiO_2 in SiMn slags can be described by using the rate models of Equations [3] and [4]. The comparisons between the rate models and the measured amount of MnO and SiO_2 between 1500 and 1650°C are described in Figure 8. Note that the parameters that describe the optimal fit were applied to the rate models (approximately 2% error in the raw materials analyses). The comparison showed that the rate models considered in this study are applicable to describe the amount of MnO and SiO_2 for SiMn slags. The symbols, which describe the measured amount of MnO and SiO_2 from

the experiments, showed a good match with the calculated amounts, solid and dotted lines, between 1500 and 1650°C. The considered rate models were successful in describing the changing amount of MnO and SiO_2 regardless of the charge-type and degree of reduction.

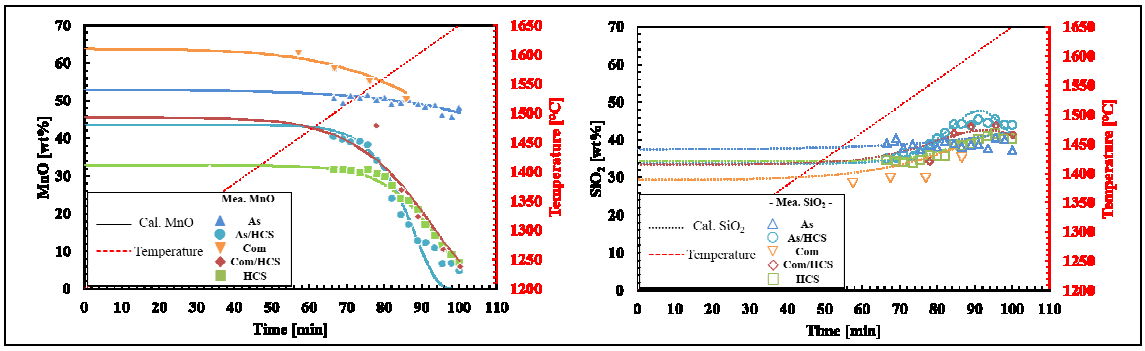

Figure 8: Comparison of calculated (solid and dotted lines) and measured (symbols) amount of MnO and SiO_2 between 1200 and 1650°C of SiMn slags

CONCLUSIONS

The objectives of this study were to estimate the kinetics of MnO and SiO_2 reduction in SiMn slags, and to observe the reduction rate between 1500 and 1650°C. The results showed that SiMn charges containing HCFeMn slag as a raw material is reduced faster than charges without. The measured amount of MnO in slag at 1650°C was low with charges containing HCFeMn slag, and the a_{MnO} showed good accordance: The a_{MnO} was around 0.2 at 1500°C, but decreased to near 0 at 1650°C. Also, the comparison of a_{MnO} at 1500°C showed values of approximately 0.2 for all charges, which implied a low contribution towards the driving force for reduction rate. From the kinetic estimations, the activation energies for charges differed in two types: For MnO reduction, some charges containing HCFeMn slag, and some without, was approximately between 500–920 and 250–300 kJ/mol, respectively. The comparison of slag viscosity with rate constants showed that slag viscosity does not significantly influence the reduction rate of MnO. Instead, a small amount of sulfur as an impurity element in the charge showed a significant impact on the reduction rates. Above 0.15 wt% of initial sulfur, the rate constants increased drastically with increasing temperatures. In addition, the considered rate models for MnO and SiO_2 reduction were able to describe the changing amount of MnO and SiO_2 in SiMn slags.

ACKNOWLEDGMENTS

This publication has been partly funded by the SFI Metal Production (Centre for Research-based Innovation, 237738). The authors gratefully acknowledge the financial support from the Research Council of Norway and the partners of the SFI Metal Production.

REFERENCES

FactSage 7.0 (CRCT: Canada, GTT: Germany)
www.factsage.com

Holtan J. 2015. Phase composition in Comilog charges during heating and reduction, Internal report: TMT 4500 Materials Technology, Specialization Project, Norwegian University of Science and Technology.

International Manganese Institute
www.manganese.org

Kawamoto R. 2016. Effect of sulfur addition on reduction mechanism of synthetic ore, Internal report: TMT 4500 Materials Technology, Specialization Project, Norwegian University of Science and Technology.
Kim P., Holtan J., and Tangstad M. 2016. Reduction behavior of Assmang and Comilog ore in the SiMn process, The 10th International Conference on Molten Slags, Fluxes and Salts (MOLTEN 16), pp.1285–1292.
Kim P., Larrsen T., Tangstad M., and Kawamoto R. 2017. Empirical activation energies of MnO and SiO_2 reduction in SiMn slags between 1500 and 1650°C, The Minerals, Metals & Materials Society 2017 (TMS 2017), pp.475–483.
Kim P. and Tangstad M. 2018*. The effect of sulfur content on the reduction rate in SiMn slags, Metall. Trans. B (To be published).
Kim P. and Tangstad M. 2018*. The effect of sulfur for MnO and SiO_2 reduction in synthetic SiMn slag, Metall. Trans. B (To be published).
Kim P. and Tangstad M. 2018*. Melting behavior of Assmang ore and quartz in the SiMn process, Metall. Trans. B (To be published).
Larrsen T.A. 2016. Reduction of MnO and SiO_2 from Comilog-based charges, Internal report: TMT 4500 Materials Technology, Specialization Project, Norwegian University of Science and Technology (NTNU).
Maroufi S., Ciezki G., Jahanshahi S., Shouyi S., and Ostrovski O. 2015. Dissolution of silica in slag in SiMn production, *Infacon XIV: The Fourteenth International Ferroalloys Congress*, Kyiv, Ukraine, 1–4 June 2015, pp. 479-487.
Olsen H. 2016. A theoretical study on the reaction rates in the SiMn production process, Master's Thesis, Department of Materials Science and Engineering, Norwegian University of Science and Technology (NTNU).
Olsen S.E., Tangstad M., and Lindstad T. 2007. *Production of manganese ferroalloys*, Tapir Academic Press, Trondheim, Norway.
Ostrovski O., Olsen S.E., Tangstad M., and Yastreboff M. 2002. Kinetic modelling of MnO reduction from manganese ore, *Canadian Metallurgical Quarterly*, Vol.41, No.3, pp.309–318.
Outotec: HSC Chemistry 7
www.hsc-chemistry.com
Skjervheim T. Kinetics and mechanisms for transfer of manganese and silicon from molten oxides to liquid manganese metal, PhD Thesis, Department of Metallurgy, The Norwegian Institute of Technology (Currently NTNU).
Stølen S. and Grande T. 2004. *Chemical thermodynamics of materials*, Wiley, West Sussex, UK.
Subramanyam D.K., Swansiger A.E., and Avery H.S. 1990. Austenitic manganese steels in properties and selection: Irons, steels and high-performance alloys, 10th ed., Ohio, ASM International.
Tomota Y., Strum M., and Morris Jr. J. 1987. The relationship between toughness and microstructure in Fe-high Mn binary alloys, *Metall. Trans. A.*, Vol.18A, pp.1073–1081.
Tranell G., Gaal S., Lu D., Tangstad M., and Safarian J. 2007. Reduction kinetics of manganese oxide from HCFeMn slags, Infacon XI, New Delhi, India, 18–21 February 2007, pp.231–240.

Pyunghwa Peace Kim
PhD Candidate, Norwegian University of Science and Technology (NTNU)

- From Seoul, South Korea
- BSc: University of Seoul (Materials Science and Engineering)
- MSc: Norwegian University of Science and Technology (Materials Science and Engineering)